29th EPS Conference on Plasma Phys. and Contr. Fusion Montreux, 17-21 June 2002 ECA Vol. **26B**, P-5.096 (2002)

Two Dimensional Soft-X ray and AXUVD Tomography Based on Magnetic Flux Surfaces

Y. Liu[1], A.Yu.Kostrioukov[3], K. Nagasaki[2], Y. D. Pan[1], B.J.Peterson[3]

[1]South Western Institute of Physics, Chengdu, China

[2]Institute of Advanced Energy, Kyoto University, Japan

[3]National Institute for Fusion Science, Japan

1. Introduction

A tomographic algorithm taking magnetic flux surfaces into account is used to reconstruct an emission image. Improvement of the quality of reconstructed images has been obtained using a feedback technique to compensate numerical errors. This tomography technique has been applied in soft x-ray measurements on HL-1M Tokamak and Heliotron J, and used for plasma radiation imaging on the Large Helical Device (LHD)[1] by using AXUVD (bolometer like semi conductive detectors) arrays [2].

2. Method used for soft X-ray and bolometric inversion

2.1 Dividing and expansion under the basis of vacuum flux surfaces

The basic principle of tomography is to reconstruct the emitted radiation from a plasma cross-section along a large number of collimated chord measurements. The reconstruction algorithm employed here is so-called hybrid methods [3]. We divide the emitting region into annular areas under the basis of real magnetic flux contours. These annular areas can be considered as pixels, as shown in Fig.1. Line integrals $f(p_i,\varphi_i)$ can accurately be represented by a summation of the contribution, g_k, from each pixel along the line of sight

$$f(p_i,\varphi_i) = \int_{L_i} g(r,\theta)dL \approx \sum_k a_{ik} g_k \qquad (1)$$

where p is the distance from the origin to the tangential point of line of sight to the corresponding surface, the chord angle φ is the polar co-ordinate of the point of tangency. Equation (1) is equivalent to have chosen a series of piecewise linear functions to represent the detected signals. These functions vanish at plasma boundary, i.e., they satisfy the basic requirement of orthonormality in the same way as Bessel functions. The local emissivity in a pixel, g_k, can be solved by using a 'peeling away' technique given in Ref [4].

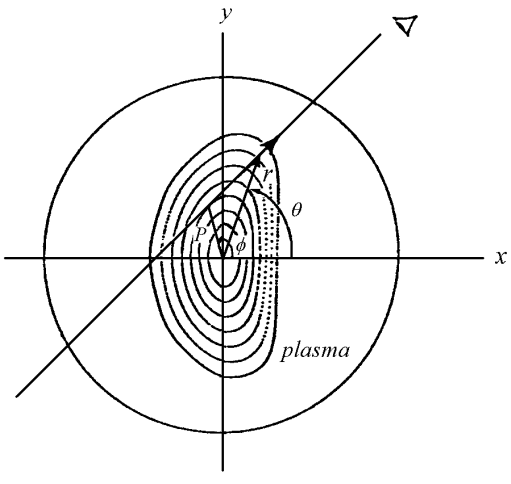

Fig.1. Co-ordinate system for reconstruction of a 2-D image. The emitting region can be divided into annular pixels with real magnetic surfaces.

To model the variation of emissivity within a pixel in the angular direction, we expand the emissivity on each pixel in Fourier

series. Then the local emissivity within a pixel is:

$$g_k = g_{k0} + \sum_m \; g^s_{km} \sin m\theta \; + g^c_{km} \cos m\theta \qquad (2)$$

The number of observation directions limits the number of Fourier modes. Higher modes as far as $\sin 2\theta$ mode are neglected if two existing arrays are used.

2.2 Feedback technique

To reduce the error and prevent the error from propagating into the inner pixel, we use a feedback technique to compensate for the error at each pixel. Since the Radon transform for emission (Eq.(1))is linear, if the inversion procedure is represented by the operator $\Re$, such that $g=\Re(f)$, the pseudo signals recalculated from the reconstructed emissivity function g' is given by $f' = \Re^{-1}(g')$, then:

$$g' - g = \Re(f') - \Re(f) = \Re(f' - f) \qquad (3)$$

This leads to a more accurate solution:

$$g = g' - \Re(f' - f) \qquad (4)$$

In other words, the difference between the measured and reconstructed line-integrated signals is fed back as an input data for the inversion process. If the reconstruction itself is stable, the feed back process makes the difference between experimental and reconstructed chord integrated data negligible.

3. Numerical Test

The technique of the reconstruction is examined numerically using a perturbed structure. The source function has a circular hot spot over flat region in the center [5].

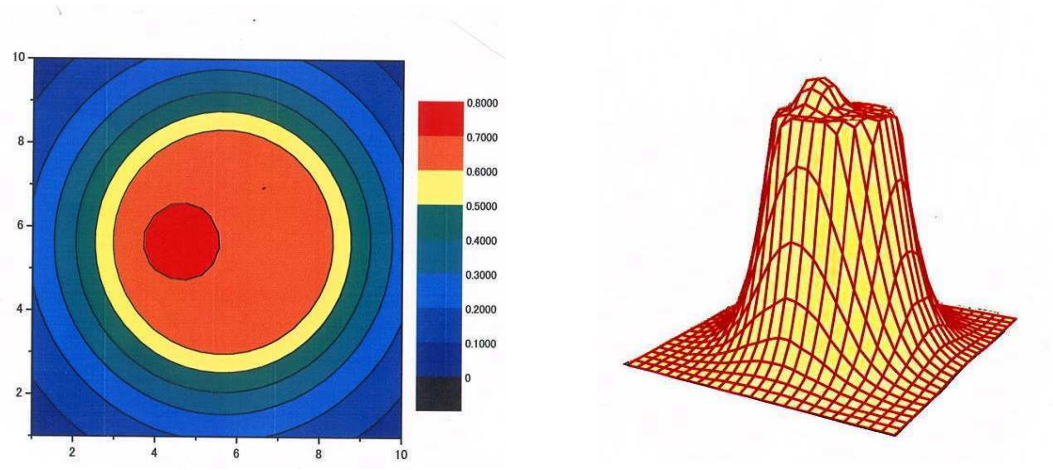

Fig.2. (a) Contour plot of the test source function and (b) surface plot of the reconstructed image.

Fig.2 shows the contour plot of the test source function and the hidden-line perspective plot of the reconstructed image for the case of small size hot spot ($r_{spot} \approx 10\%$ of r_s).

4. Application to AXUVD measurement on LHD

Fig.3 shows two AXUVD arrays (20 channels each) installed on a semi-tangential cross-section in LHD. Part of the emitting volume was only seen from the right side (4-O array). The plasma shape strongly depends on the magnetic axis position, R_{ax}. For smaller R_{ax}, the part not seen from above was bigger, which made the tomography procedure more difficult. In addition, high spatial resolution requirement near the boundary, strong poloidal asymmetries in radiation distribution and the far deviation from circular shape in the edge region make a serious challenge for the inversion technology.

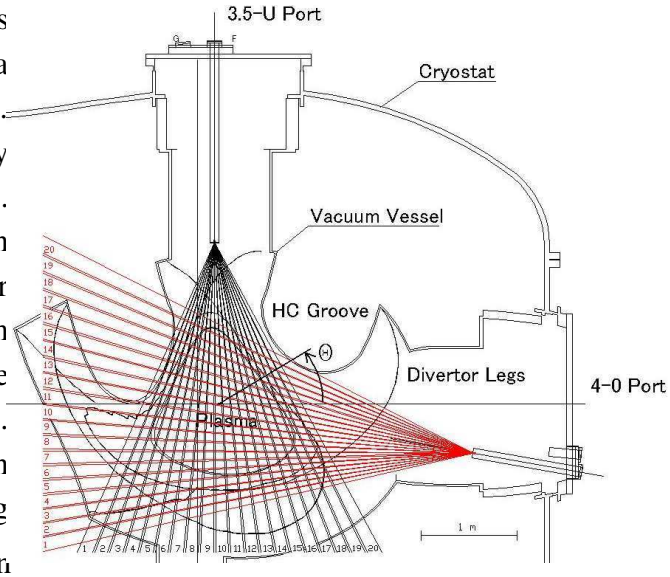

Fig.3. Lines of sight of the bolometric tomography on LHD.

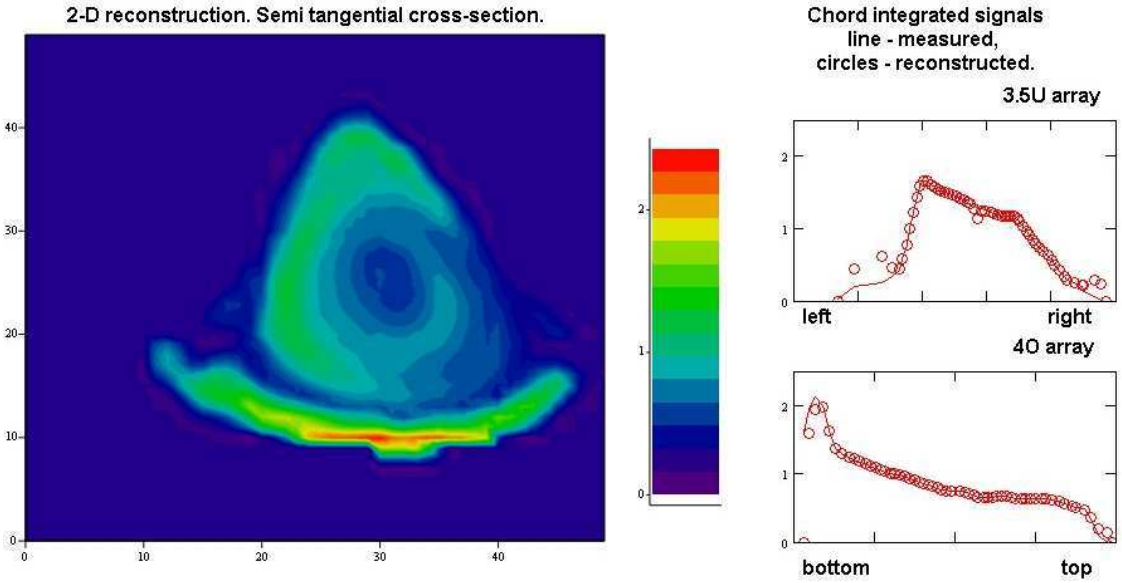

Fig. 4. 2-D bolometric emissivity profile reconstruction in Shot 31721 t=2 s. The bright region at the bottom is due to 3.5L gas puffing .

The tomography algorithm described above provided reasonable two-dimensional profiles of plasma emission and a good agreement between experimental and simulated chord integrated emission for different conditions. Fig.4 shows a hollow profile with additional peripheral emission caused by the gas puffing from the bottom nozzle. Small differences between reconstructed and measured chord integrated profiles (4O array) were caused by reconstruction artifacts. Fig.5 shows the emissivity for the same discharge at the moment when the gas puffing was off.

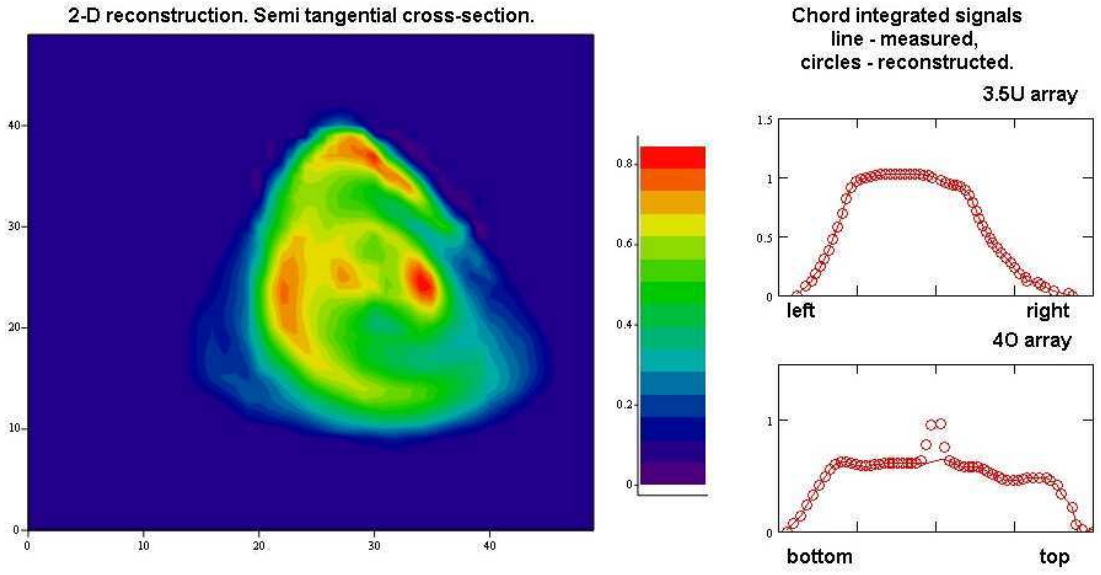

Fig. 5. 2-D emissivity bolometric profile reconstruction, shot 31721, t=3.5 s. The gas puffing was off.

5. Discussion

The main advantage of the method employed is that the boundary condition is naturally met by solving the equation in the outermost pixel. Taking the complicated real plasma shape into account makes the algorithm start from a grid that is closer to the true plasma radiation contours. It is suitable to be applied in measurements of soft x ray and total radiation on the LHD and Heliotron J with widely arbitrary cross sections. Furthermore, we modified this tomographic algorithm with a feedback procedure. As a result, the 2-D technique was powerful enough to provide reasonable images in the most of the cases. However, since the number of detector arrays is limited, only a finite number of Fourier components can be used in the expansion. In some cases (strong asymmetry or contours of constant radiation emissivity deviate far from magnetic flux surfaces) the reconstruction was not so reasonable, i.e. the difference between experimental and reconstructed chord integrated data drastically diverges in the central part of the image.

6.Conclusions

Numerical test and the results of the 2-D tomography technique applied to the experimental data showed that the algorithm is powerful enough to reconstruct complicated asymmetric emissivity distribution.

References

[1] A.Komori et al., Plasma Phys. Control Fusion 42 (2000) 1165.
[2] A.Yu.Kostrioukov et al., Submitted to Rev. Sci. Instrum., 2002.
[3] P.Smeulders, Nucl.Fusion 26, 267 (1986).
[4] R.S.Granetz, P.Smeulders, Nucl.Fusion28, 457 (1988)
[5] Y.Nagayama et al., Rev.Sci.Instrum.65, 3415 (1994)